DEPARTMENT OF THE INTERIOR
U.S. GEOLOGICAL SURVEY

MISCELLANEOUS INVESTIGATIONS SERIES
MAP I–1257–E

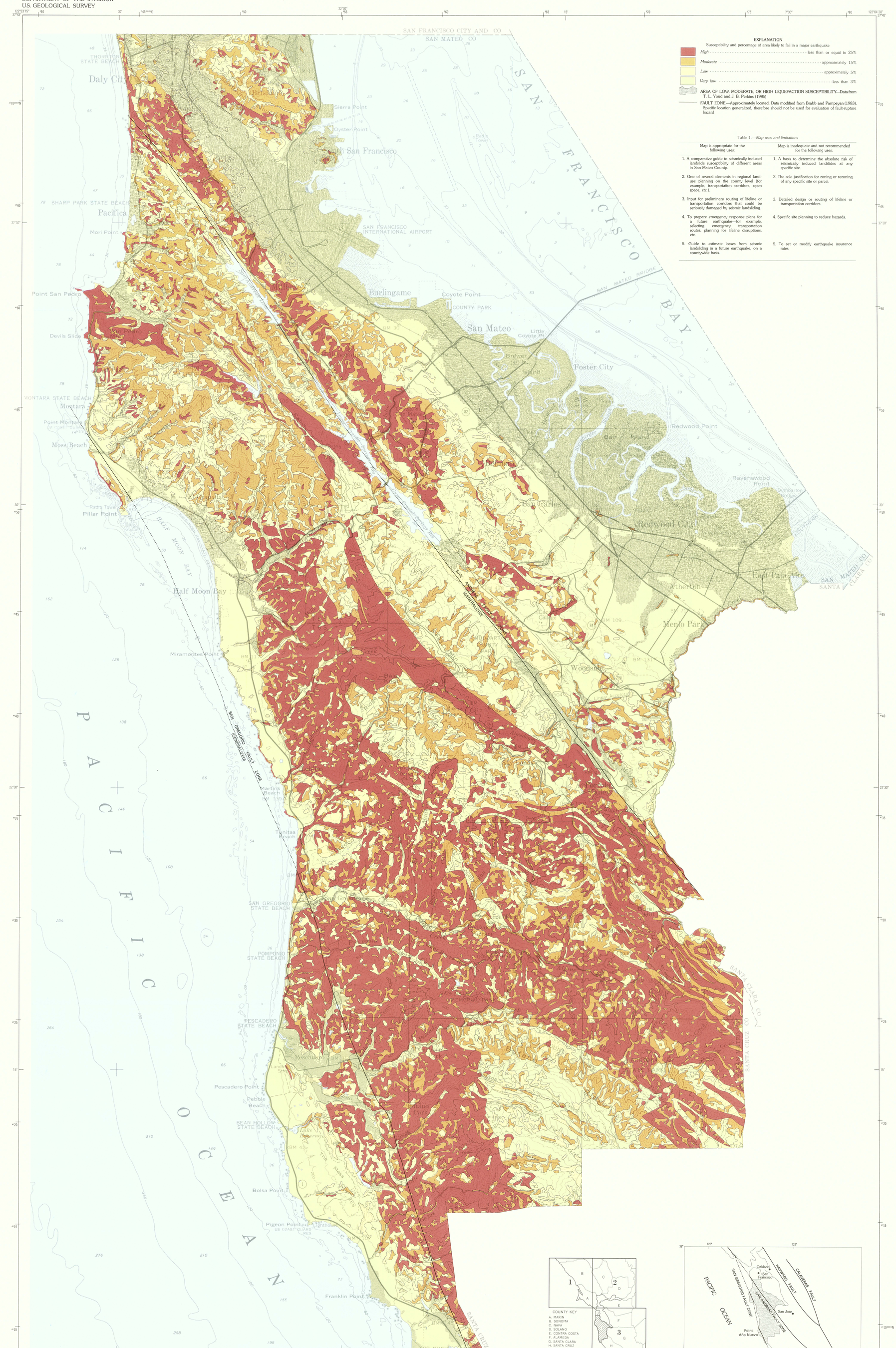

Base from U.S. Geological Survey, San Francisco Bay Region, sheet 3, 1:125,000, 1970. Park boundaries revised 1981.

5000-meter Universal Transverse Mercator grid ticks, zone 10

APPROXIMATE MEAN DECLINATION, 1980

SCALE 1:62 500

CONTOUR INTERVAL 200 FEET
DOTTED LINES REPRESENT 40-FOOT CONTOURS
NATIONAL GEODETIC VERTICAL DATUM OF 1929
DEPTH CURVES IN FEET–DATUM IS MEAN LOWER LOW WATER
SHORELINE SHOWN REPRESENTS THE APPROXIMATE LINE OF MEAN HIGH WATER
THE MEAN RANGE OF TIDE IS APPROXIMATELY 4 FEET IN THE PACIFIC OCEAN And 5 FEET IN SAN FRANCISCO BAY

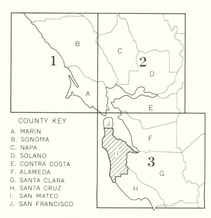

INDEX MAP SHOWING AREA OF THIS REPORT

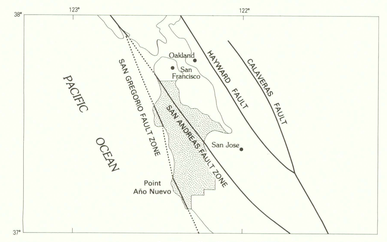

INDEX MAP SHOWING APPROXIMATE LOCATION OF MAJOR FAULTS IN THE SAN FRANCISCO BAY AREA, SAN MATEO COUNTY SHOWN BY PATTERNED AREA

INTERIOR—GEOLOGICAL SURVEY, RESTON, VA.—1985—GS/47

Susceptibility criteria compiled in 1978–79.

EXPLANATION

Susceptibility and percentage of area likely to fail in a major earthquake

- *High* ..... less than or equal to 25%
- *Moderate* ..... approximately 15%
- *Low* ..... approximately 5%
- *Very low* ..... less than 3%

AREA OF LOW, MODERATE, OR HIGH LIQUEFACTION SUSCEPTIBILITY—Data from T. L. Youd and J. B. Perkins (1985)

FAULT ZONE—Approximately located. Data modified from Brabb and Pampeyan (1983). Specific location generalized, therefore should not be used for evaluation of fault-rupture hazard

Table 1.—Map uses and limitations

Map is appropriate for the following uses:	Map is inadequate and not recommended for the following uses:
1. A comparative guide to seismically induced landslide susceptibility of different areas in San Mateo County.	1. A basis to determine the absolute risk of seismically induced landslides at any specific site.
2. One of several elements in regional land-use planning on the county level (for example, transportation corridors, open space, etc.).	2. The sole justification for zoning or rezoning of any specific site or parcel.
3. Input for preliminary routing of lifeline or transportation corridors that could be seriously damaged by seismic landsliding.	3. Detailed design or routing of lifeline or transportation corridors.
4. To prepare emergency response plans for a future earthquake—for example, selecting emergency transportation routes, planning for lifeline disruptions, etc.	4. Specific site planning to reduce hazards.
5. Guide to estimate losses from seismic landsliding in a future earthquake, on a countywide basis.	5. To set or modify earthquake insurance rates.

INTRODUCTION

This map of slope stability during earthquakes for San Mateo County, Calif., identifies potentially hazardous areas by indicating zones which have *very low, low, moderate,* or *high* susceptibility to seismically induced landsliding; its purpose is to help minimize loss of life and damage. Susceptibility is evaluated from a technique which utilizes lithologic, hydrologic, slope and seismic data. Because the estimated susceptibility of each zone is based on limited data within each geologic unit, the map is not adequate or valid for determination of susceptibility at any specific site. However, the map does delineate areas where the probability of landsliding during a major earthquake is greatest and where special attention is required when considering general land-use planning.

Seismically induced landslides are responsible for a substantial portion of loss of life and property damage during earthquakes, so methods to identify susceptible landslide areas are important for seismic-hazard awareness. This is critical in the San Francisco Bay area, given the seismic history, the abundance of landslides, and the strong pressure for development. San Mateo County, in particular, has a history of seismically induced landslides (Youd and Hoose, 1978), is traversed by several active faults including the San Andreas, and is likely to experience future large earthquakes. A method to identify hazardous areas has been developed and applied here to depict relative susceptibility to seismic slope failures on a regional scale of 1:62,500.

Criteria used in producing the map include slope steepness, average material properties, and estimated seismic ground motions. Criteria for evaluating seismic slope stability, at the scale of this map, were developed by combining a static slope-stability analysis with a dynamic numerical analysis developed by Newmark (1965). The slope-stability analysis utilizes regional geologic, hydrologic, and slope information to evaluate slope stability under static conditions. Strong-motion records from several California earthquakes were used to choose hypothetical (or "design") earthquakes large enough to trigger landslides in San Mateo County. These "design" earthquakes were used in the dynamic analysis to calculate movement of potential landslides. These movements were then used to categorize the geologic map into four degrees of susceptibility.

This map is designed to aid planners, building officials, engineers, geologists, and interested private citizens concerned with identifying areas susceptible to landsliding during earthquakes in San Mateo County. Because of this wide spectrum of potential users, the text is divided into a discussion of the uses and limitations of the map, followed by an explanation of the method used to compile the map.

MAP USES AND LIMITATIONS

The seismic slope-stability map has a variety of uses on a regional scale, ranging from land-use planning to preliminary route selection of transportation and other lifeline corridors, as listed in table 1. It is inadequate or may even be misleading for other purposes, and is not appropriate for specific uses at individual sites, due to limitations of scale, data, and analysis.

It is important to reemphasize some of the map's limitations. This map was prepared at a scale of 1:62,500 (1 inch approximately equals 1 mile) to be compatible with two source maps—the geologic map (Brabb and Pampeyan, 1983) and an unpublished slope map of San Mateo County—as well as to represent the entire county in a convenient format. As a result the map lacks sufficient detail for evaluation of the susceptibility to seismic landsliding at any particular site or tract. An exact evaluation of the risk of seismically induced slope failures at specific sites requires geologic and geotechnical investigations that are much more detailed than those appropriate for these regional interpretations.

Inadequacies in the unpublished slope map, on which some of our data is based, imposed certain limitations on preparation of the stability map. The 1:62,500 slope map, prepared by a photomechanical process from 1:24,000 topographic maps with 40-foot contour intervals, is divided into six slope intervals: (I) 0-5 percent, (II) 5-15 percent, (III) 15-30 percent, (IV) 30-50 percent, (V) 50-70 percent, and (VI) greater than 70 percent. Because of difficulties in preparation and compilation, the 1:62,500 slope map underestimates steep slopes in some small areas such as along some stream banks, landslide scarps, road cuts, and sea cliffs; we have attempted to adjust this data by separately identifying these areas from the 1:24,000 topographic maps.

Another limitation of our map is that the analysis of seismic slope stability requires lithologic delineation in terms of material strength rather than in terms given on standard geologic maps such as age and stratigraphy. So as not to underestimate the landslide susceptibility at any place within a geologic unit, we assigned material strengths on the basis of the weakest rock type present in the unit. For example, chert of the Franciscan assemblage (unit fc, table 3), which consists of chert interbedded with shale, was assigned a strength on the basis of the presence of a weak shale member. Conservative estimates of strength were necessary because individual testing of each of the 53 geologic units in San Mateo County was impractical; consequently, many areas in the county actually underlain by stronger materials are thus slightly less susceptible to failure than the map indicates.

Two values for pore-water pressure were assumed as extremes of the seasonal ground-water level, since during the majority of the year, the ground-water level generally fluctuates between these two conditions. On the map, separate susceptibility categories indicate slopes where the ground-water conditions effected the seismic slope stability. An increase in pore-water pressure during shaking and any subsequent reduction in slope stability were not considered in the analysis for the preparation of the map. This limitation may result in the underestimation of the susceptibility of some areas underlain by highly permeable, saturated materials to seismically induced landsliding.

This study did not consider liquefaction or particular types of landslides, wet-sand flows and lateral spreads, that commonly occur as a result of liquefaction; so therefore, the map does not show susceptibility to these particular types of landslides. Areas of San Mateo County which may have low, moderate, or high susceptibility to liquefaction as determined by T. L. Youd and J. B. Perkins (1985) are shown with a stippled pattern on our map.

Table 2 gives rough estimates of the percentage of each susceptibility zone that we would expect to fail in a major earthquake, such as a repeat of the 1906 San Francisco earthquake or a earthquake greater than 8 on the Richter scale. These estimates were prepared from an examination of the percentage of area involved in slope failures in areas of strong ground shaking during historical earthquakes in San Mateo County (Youd and Hoose, 1978) and in other areas (Garwood and others, 1979; Harp and others, 1981). These estimates indicate relative levels of risk within various susceptibility zones.

Table 2.—Estimated failure within susceptibility zones

Susceptibility zone	Percentage of area likely to fail in a major earthquake
High	less than or equal to 25%
Moderate	approximately 15%
Low	approximately 5%
Very low	less than 3%

COMPILATION PROCEDURE

The most abundant seismically induced landslides are falls, slides, block slides and slumps of soil and rock, and lateral spreads in soils (Keefer, 1984; Keefer and others, 1978; classification of types of slope movement according to Varnes, 1978). Because rock and soil falls appear to be initiated by tensile failure only on the steepest slopes (Sitar and Clough, 1983; Harp and others, 1981), falls were treated separately from the other types of ground failure by conservatively indentifying slopes steeper than 70 percent as highly susceptible to falls.

Lateral spreads and wet-sand flows result from the process of liquefaction, and we relied on the liquefaction-susceptibility evaluation of T. L. Youd and J. B. Perkins (1985), to indentify areas susceptible to these types of ground failure. Slides, block slides, and slumps were evaluated using the dynamic numerical analysis developed by Newmark (1965), to categorize their susceptibility to movement during earthquakes.

STATIC SLOPE–STABILITY ANALYSIS

The first step in calculating the potential movement of a landslide during an earthquake is to evaluate the Factor of Safety (F.S.) of the slope under static conditions; the Factor of Safety is an index that is defined as the ratio of the total force available to resist sliding to the total static force tending to induce sliding (Hoek and Bray, 1977, p. 27). Many methods of slope-stability analysis have been developed for evaluation of the F.S. for individual sites; however, for analyzing slope stability of San Mateo County at a scale of 1:62,500, we needed a method that could be used regionally. An infinite slope analysis (Skempton and Hutchinson, 1969; Dunn and others, 1980, p. 240) was selected because the method is simple to apply, gives a generally conservative result, and is adequate for our level of precision.

An infinite slope analysis is appropriate if the potential landslide is thin in comparison to its length, if the failure surface is parallel to the slope, and if failure takes place by basal shearing (Lambe and Whitman, 1969, p. 192). The potential landslide is also assumed to act as a rigid friction block (fig. 1). The assumption of rigidity is applicable so long as the slide, block slide, or slump moves by translation and (or) rotation with minimal internal disruption. The infinite slope analysis is applicable to slides and block slides because all the above conditions are satisfied. However, for slumps, which do not have a failure surface parallel to the slope, the results of the infinite slope analysis are still reasonably applicable for the purposes of our analysis, so long as the slump occurs along a relatively uniform slope. Near cliffs and other sharp topographic breaks, the upper portion of a slump may incorporate a portion of the relatively flat surface upslope of steeper slopes. In such cases, the infinite slope analysis would overestimate the stability of the flat area upslope. The problem of identifying the susceptibility to landsliding of flat areas adjacent to steep slopes using regional slope maps has been recognized by Brabb and others (1972). For site-specific studies the problem could be addressed by selecting appropriate setbacks from steep slopes. For example, based on the experience of seismically induced landsliding in Guatemala City during the 1976 earthquake, setbacks of 10 m (34 ft) from steep slopes were suggested (Harp and others, 1978, p. 364). However, at the scale of 1:62,500, such setbacks would not significantly alter our map, and therefore we considered the infinite slope analysis sufficiently accurate even for slumps near sharp topographic breaks.

In an infinite slope analysis the F.S. can be expressed as the ratio of the maximum shearing resistance, R (equal to the shear strength multplied by the area of sliding surface), to the downslope component of the gravitational load, L (equal to the mass multiplied by the acceleration of gravity times the sine of slope angle). Thus, the F.S. of the landslide illustrated as a rigid friction block in figure 1 may be represented in terms of effective stress as:

$$F.S. = R/L = \frac{(c'A + (mg\cos\theta - uA)\tan\phi')}{mg\sin\theta} \qquad (1)$$

where c' is the effective cohesion, A is the area of the sliding surface, m is the mass of the landslide, g is the acceleration due to gravity, θ is the slope angle, u is the pore-water pressure on the sliding surface, and ϕ' is the effecive friction angle.

Strength Parameters

We divided the geologic units of San Mateo County (as defined by Brabb and Pampeyan, 1983) into three categories shown in table 3: (A) crystalline rocks and well-cemented sandstones, (B) unconsolidated and weakly cemented sandstones, and (C) shales and clays. These categories were assigned on the basis of detailed lithologic description (Stephen Ellen and others, *in* Brabb and Pampeyan, 1972b); downhole geophysical testing of seismic velocities near the surface in shallow boreholes in these units (Gibbs and others, 1977); field examination of outcrops noting frequency, spacing, orientation, and strength of discontinuities such as bedding planes, joints, foliations, etc.; and laboratory shear and tensile strength tests. Areas identified as definite and probable landslide deposits in San Mateo County (Brabb and Pampeyan, 1972a) were assigned to Category C.

Average values of effective shear-strength parameters, c' and ϕ', were estimated for each category on the basis of a limited number of direct shear tests of some units, from unpublished strength data on file with the San Mateo County geologist in Redwood City, Al Neufeld (written commun., 1981), and strengths of similar soils and rocks measured elsewhere (Hoek and Bray, 1977, p. 23, 115; Underwood, 1967, p. 112; and Dearman and others, 1978). The relatively low values of c' and ϕ' listed in table 4 were selected to represent average shear strengths within several meters of the surface in the zones including residual and colluvial soils as well as extensively weathered and fissured rock. The crystalline rocks and well-cemented sandstones were assigned the highest shear strength—a friction angle of 35° with a cohesion of 14.4 kN/m^2 (300 lb/ft^2). Unconsolidated and weakly cemented sandstones were assigned an intermediate strength—a friction angle of 35° with zero cohesion. Shales and clays were assigned the lowest strength—a friction angle of 20° with zero cohesion.

No cohesion was assigned to shales and clays because the shale units in San Mateo County are deeply weathered and fissured within several meters of the surface and hence have minimal cohesion within the rock mass. By assigning zero cohesion to unconsolidated and weakly cemented sandstones as well as shales and clays, we may have underestimated the cohesive strength of materials on some hillsides, but thought this preferable to overestimating the cohesion in most situations, particularly in light of the recognized fact that cohesion in these types of materials fluctuates seasonally as a function of water content.

Where a geologic unit consists of two or more members of differing lithologies, the entire unit was assigned to a category based on the weakest lithology. Using such strengths in the infinite slope analysis results in a conservative F.S., lower than might actually exist. However, due to possible strength variation within a single geologic unit, a low shear-strength value was considered appropriate.

Table 4.—Estimates of strength for categories of geologic units in, San Mateo County

Categories of geologic units	Effective shear-strength parameters	
	ϕ'	c'
A	35°	14.4 kN/m^2(300 lb/ft^2)
B	35°	0
C	20°	0

If *mg* is replaced by γhA, equation 1 reduces to

$$F.S. = (c'/\gamma h\sin\theta) + \cot\theta\tan\phi' - (u\tan\phi'/\gamma h\sin\theta), \qquad (2)$$

where γ is the unit weight of the potential landslide mass and h is its thickness (measured perpendicular to the slope as shown in fig. 1). In the first term of equation 2, we assumed γ equal to 1,602 kg/m^3 (100 lb/ft^3) and h equal to 3 m (10 ft). This unit weight was based on typical values for soils and weathered rocks (Hoek and Bray, 1977, p. 23). We assumed an average landslide thickness of 3 m (10 ft), based on observations of the depth of weathering in San Mateo County. Keefer (1984) has shown that the most abundant seismically induced landslides are "shallow", generally less than 3 m (10 ft) below the surface in residual and colluvial soils or weathered, sheared, or closely jointed bedrock.

Hydrologic Parameters

On the basis of measured ground-water-level fluctuations on slopes in San Mateo County (Wieczorek, 1978, 1981), two general ground-water conditions were specified for this report. The ground-water level was assumed to be greater than 3 m (10 ft) deep (below the design thickness of the landslide) during the dry summer and fall seasons. During the wet winter and spring seasons the ground-water level was assumed to be at the surface, with fully saturated flow parallel to the surface. These two general conditions were used to approximate pore-water pressures in equation 2. For the dry condition, that is when u = 0, equation 2 reduces to

$$F.S. = (c'/\gamma h\sin\theta) + \cot\theta\tan\phi'. \qquad (3a)$$

For the wet condition the pore-water presure on the slide plane (u) is equal to $\gamma_w h\cos\theta$ and equation 2 reduces to

$$F.S. = (c'/\gamma h\sin\theta) + [1-(\gamma_w/\gamma)]\cot\theta\tan\phi', \qquad (3b)$$

where γ_w is the unit weight of water, 1,000 kg / m^3 (62.4 lb/ft^3).

SELECTION OF DESIGN EARTHQUAKES

The seismicity of San Mateo County and the historical record of earthquakes, which have caused landsliding, were examined to select design earthquakes appropriate for San Mateo County. The San Andreas fault in this area has shown activity in historical earthquakes, with fault rupture reported in 1836 and 1906. The San Gregorio fault is considered active because of offsets to geologic units during middle and late Pleistocene time (Lajoie and others, 1979). In addition several other active faults within the San Francisco Bay area are capable of large-magnitude earthquakes (Herd, 1978) which could cause strong ground shaking in the county.

As a measure of the severity of seismic shaking necessary to trigger landsliding, strong-motion records of several California earthquakes were compared, using a technique developed by Newmark (1965), to analyze movements of earth dams and embankments during earthquakes. Seed and Goodman (1964) adapted this method to analyze the seismic stability of slopes with cohesionless soils, and Sarma (1975) further developed the method to accommodate dynamic pore-water pressures generated during an earthquake. Although we did not consider dynamic pore-water pressure effects or the effect of a reduction in strength during movement of the landslide, we have extended the method to include natural slopes of both cohesive and cohesionless materials with static pore-water pressures and have expanded the application to a regional scale.

A yield or critical acceleration, a_c, required to overcome slope equilibrium along a sliding surface was derived from Newmark (1965, p. 152, eq. 20) by multiplying each side of his equation by g, the acceleration due to gravity, to yield

$$a_c = (F.S. - 1)\, g\sin\theta \qquad (4)$$

where a_c is parallel to the slope and measured in terms of g, the acceleration due to gravity, and F.S. is the Factor of Safety under static, nonseismic conditions. However, because small irreversible slope movements during an earthquake do not necessarily result in a landslide, the amount of slope movement must be determined. Based on the technique developed by Newmark (1965), the movement of the landslide along an assumed planar failure surface is calculated from an algorithm (Wilson and Keefer, 1983) that determines the movement of a rigid friction block subjected to an acceleration-time history corresponding to a seismic strong-motion record. An example of this process is illustrated in figure 2, a plot of acceleration versus time for an actual strong-motion record. Superimposed on this strong-motion record is a horizontal line corresponding to the critical acceleration of a particular slope (a_c = 0.2 g in this example). The first step is to integrate those portions of the strong-motion record which lie above the critical acceleration. The integration begins at point A in figure 2*A* where the ground acceleration first exceeds a_c. We integrate that portion **AB** of the ground motion above a_c, over time, to calculate the velocity of the block (fig. 2*B*). At point **B**, the block reaches the maximum velocity for this acceleration pulse. After point **B**, when the ground acceleration drops below the critical acceleration, the block is still in motion due to its inertia, but is now being decelerated by the friction which still exists beneath the block. Also the ground acceleration may well swing around in the opposite direction and directly oppose the motion of the block. Eventually, the motion of the block will cease and the block will come to rest at point **C**. Finally, the movement of the block is calculated by integrating the velocity of the block over time (fig. 2*C*). In this example, there is also a second pulse of ground acceleration exceeding a_c from points **D** to **E** in figure 2*A*, producing a second increment of movement which ends with a small movement in the upslope direction from points **F** to **G** in figure 2*C*, slightly reducing the total movement of the block in the downslope direction. Although small movements in the upslope direction are possible, they are difficult because the critical acceleration in the upslope direction is much greater than in the downslope direction. Except on very flat slopes, the total downslope movement will exceed any incremental upslope movements.

By performing this calculation for different values of a_c, it can be seen than as a_c is lowered, more of the smaller peaks on the record are intergrated, and the movement increases. No movement occurs if a_c is not exceeded by the peak acceleration during the earthquake. Thus for higher values of a_c, the peak acceleration is the most important parameter; for lower a_c, the duration of shaking becomes more significant.

For any strong-motion record, displacements may be calculated for a variety of a_c values representing a variety of combinations of different degrees of slope and different strengths of materials. A log/log plot of landslide movement versus a_c is useful for comparing the effect of different ground motions on movement. The plots shown in figure 3 (hereafter referred to as earthquake displacement curves) for several southern California strong-motion records were used to bracket landslide movement for different earthquakes which might be expected in San Mateo County.

The Taft record of the 1952 M_S=7.7 (magnitude 7.7 on the Richter scale) Arvin-Tehachapi earthquake (Neumann and Cloud, 1955), which was recorded approximately 35 km (22 mi) from the surface rupture, represents a far-field record of a major earthquake. Numerous landslides were observed in the vicinity of the fault break (Buwalda and St. Amand, 1955), but none were reported in the hills near Taft. The Taft record was selected as a level of shaking insufficient to trigger widespread landsliding during a major far-field earthquake. The Pacoima S. 16° E. record from the 1971 M_S=6.4 San Fernando earthquake (Trifunac and Hudson, 1971), which was recorded approximately 5 km (3 mi) from the surface rupture, represents one of the strongest near-field records to date. The shaking was strong enough to trigger thousands of landslides in the mountains near the Pacoima site (Morton, 1975). The Parkfield Station 2 N. 65° E. record of the 1966 M_S=5.5 Parkfield earthquake (Housner and Trifunac, 1967) and the El Centro record of the 1940 M_S=7.0 Imperial Valley earthquake (Ulrich, 1941) are included in figure 3 because they are well-known records in the field of earthquake engineering and represent near-field records of moderate and major earthquakes.

The wide range between the Taft and Pacoima earthquake displacement curves in figure 3 represents a wide spectrum of possible earthquakes. Within this range, lower-bound and upper-bound curves have been selected. The lower-bound curve, slightly higher than the Taft record, approximates a far-field record from a major earthquake or a near-field record of a moderate earthquake sufficient to trigger landsliding. For San Mateo County, an M_S = 6 earthquake on the San Andreas or San Gregorio faults or an M_S = 7 on the Hayward or Calaveras faults with epicenters in the San Francisco Bay area would represent near-field moderate earthquakes. The upper-bound curve models a near-field record of a major earthquake on a strike-slip fault, thus representing a repetition of the 1906 San Francisco earthquake (estimated surface-wave magnitude M_S = 8.2-8.3). Note that the upper-bound curve depicted in figure 3 lies below the Pacoima curve. This upper-bound curve represents a lower expected peak acceleration (0.75 g) from a strike-slip fault mechanism than from the higher stress-drop, thrust-fault mechanism responsible for the very high peak acceleration (1.25 g) at Pacoima. The San Andreas, San Gregorio, Hayward, and Calaveras faults are expected to produce stress drops and peak accelerations similar to other strike-slip faults, in accordance with the upper-bound curve.

LANDSLIDE MOVEMENT

For the slopes of San Mateo County, a_c was evaluated by substituting the expressions for F.S. in equations 3a and b into equation 4, resulting in

$$a_c = g[(c'/\gamma h) + \cos\theta\tan\phi' - \sin\theta] \qquad (5a)$$

and

$$a_c = g\left[(c'/\gamma h) + [1-(\gamma_w/\gamma)]\cos\theta\tan\phi' - \sin\theta\right] \qquad (5b)$$

for dry and wet conditions, respectively. The variation of a_c with slope is illustrated in figure 4 for the three different lithologic categories of San Mateo County.

Depending on the type of building foundation, structures generally cannot withstand more than 10 to 30 cm (3.9 to 11.8 in.) of movement without damage if located astride a fault or margin of a landslide (Youd, 1980). Five cm (2.0 in.) was selected as a conservative design threshold for landsliding that is potentially hazardous to structures and human life.

SUSCEPTIBILITY CRITERIA

The curves in figure 3 were used to determine the movement of potential landslides for a range of possible values of a_c for the upper- and lower-bound design earthquakes. Comparison between the calculated movement and the design movement of 5 cm (2.0 in.) was used to categorize landslide susceptibility as listed in table 5. For a_c less than 0.1 g during the entire year, the movement exceeded 5 cm (2.0 in.) for the lower bound earthquake, and a *high* susceptibility was assigned. For a_c less than 0.3 g but greater than 0.1 g displacements exceeded 5 cm (2.0 in.) for the upper-bound earthquake but was less than 5 cm (2.0 in.) for the lower-bound earthquake, so intermediate ratings of *low* or *moderate* were assigned, depending on the seasonal ground-water level. As can be seen on the earthquake displacement curves in figure 3, for a_c greater than 0.3 g, the movement was less than 5 cm (2.0 in.) for the upper-bound earthquake, and therefore a *very low* susceptibility was assigned.

During the wet conditions, the rise of ground-water level decreases both the F.S. and a_c, thereby increasing the movement likely during an earthquake. Accordingly, a *low* rating was assigned to slopes for which the a_c was greater than 0.3 g during the dry conditions but a_c decreased to between 0.1 g and 0.3 g during the wet conditions. In turn, a *moderate* rating was assigned if a_c was greater than 0.1 g and less than 0.3 g during the dry conditions but a_c decreased to less than 0.1 g during the wet conditions. These criteria of susceptibility are summarized in table 5.

Table 5.—Criteria for landslide susceptibility

Seasonal ground-water-level condition	Critical acceleration (a_c)	Slope movement	Susceptibility
Wet or dry	Less than 0.1 g	Greater than 5 cm (2 in.) for lower-bound earthquake	*High*
Dry	0.1 – 0.3 g	Greater than or equal to 5 cm (2 in.) for upper-bound earthquake	*Moderate*
Dry	0.1 – 0.3 g	Less than or equal to 5 cm (2 in.) for lower-bound earthquake	*Moderate*
Wet	Less than or equal to 0.1 g	Greater than 5 cm (2 in.) for lower-bound earthquake	*Moderate*
Dry	Greater than or equal to 0.3 g	Less than or equal to 5 cm (2 in.) for upper-bound earthquake	*Low*
Wet	0.1 – 0.3 g	Greater than or equal to 5 cm (2 in.) for upper-bound earthquake	*Low*
Wet	0.1 – 0.3 g	Less than or equal to 5 cm (2 in.) for lower-bound earthquake	*Low*
Wet or dry	Greater than 0.3 g	Less than 5 cm (2 in.) for upper-bound earthquake	*Very Low*

Susceptibility criteria are determined directly from lithologic categories and percent slope (table 6). Our map showing susceptibility to seismically induced slope failures of San Mateo County was prepared using this data (table 6) and information from overlays of slope and geologic maps.

Table 6.—Susceptibility criteria for seismically induced landslides in San Mateo County
[Susceptibility. VL, *very low;* L, *low;* M, *moderate;* H, *high*]

Percent slope interval ----------	I	II	III	IV	V	VI
Lithologic category	0-5	5-15	15-30	30-50	50-70	>70
A	VL	VL	VL	VL	L	H
B	VL	VL	L	M	H	H
C	VL	L	M	H	H	H

SUMMARY

Our map shows that approximately 30 percent of San Mateo County has a *high* susceptibility to seismically induced landsliding (shown in red on the map). Most of the *high* susceptible areas are in the steep, presently undeveloped, western portion of the county. In these areas the greatest hazard may be rockfalls and rockslides that block major highways. Approximately 45 percent of the county has *very low* susceptibility (green) due to gentle slopes. However, part of this area may be susceptible to liquefaction (indicated by stippled pattern). The *low* and *moderate* susceptibility zones (orange and yellow respectively) comprise the remaining 10 percent and 15 percent of the county, respectively. Particularly during wet conditions, block slides and slumps may pose the greatest hazard to structures located in *low* and *moderate* susceptibility zones.

An estimate of the percentage of each zone expected to fail in a future major earthquake is given in table 2. These estimates were prepared from a brief examination of historical earthquakes and our own postearthquake experience. These estimates are intended to convey an idea of the relative levels of risk between the various susceptibility zones, not an absolute value of risk at any specific site. Although most failures are expected to occur in *moderate* and *high* zones, a very small number may occur in the *low* and *very low* zones.

There are several ways in which our map could be improved. Basic engineering-geologic data collected on a systematic regional basis would improve the evaluation of the static F.S. and result in a more accurate representation of the critical accelerations categorizing different combinations of slope and lithology. Maps depicting materials with similar strength characteristics, thickness of soil and weathered rock, and seasonal ground-water depths and ranges of fluctuation, such as described by the Commission on Engineering Maps of the international Association of Engineering Geology (1976), would be especially useful as basic data in the analyses.

Verification and further improvement of the analytical method will result from additional comparisons of measured landslide displacements with calculated displacements, using the Newmark (1965) analysis and strong-motion records, such as those by Wilson and Keefer (1983). It would also be highly instructive to compare the distribution of landslides in future earthquakes with susceptibility maps prepared using his method. Therefore, this method should become increasingly useful for regional seismic-hazard reduction.

REFERENCES CITED

Brabb, E. E., and Pampeyan, E. H., 1972a, Preliminary map of landslide deposits in San Mateo County, California: U.S. Geological Survey Miscellaneous Field Studies Map MF–344, scale 1:62,500.

———1972b, Preliminary geologic map of San Mateo County, California: U.S. Geological Survey Miscellaneous Field Studies Map MF–328, scale 1:62,500, 1 sheet, 10 p.

———1983, Geologic map of San Mateo County, California: U.S. Geological Survey Miscellaneous Investigations Series Map I–1257–A, scale 1:62,500.

Brabb, E. E., Pampeyan, E. H., and Bonilla, M. G., 1972, Landslide susceptibility in San Mateo County, California: U.S. Geological Survey Miscellaneous Field Studies Map MF–360, scale 1:62,500.

Buwalda, J. P., and St. Amand, Pierre, 1955, Geological effects of the Arvin-Tehachapi earthquake *in* Oakeshott, G. B., editor, Earthquakes in Kern County, California, during 1952: California Division of Mines Bulletin 171, p. 41-56.

Commission on Engineering Geological Maps of the International Association of Engineering Geology, 1976, Engineering geologic maps—a guide to their preparation: Paris, The Unesco Press, 79 p.

Dearman, W. R., Baynes, F. J., and Irfan, T. Y., 1978, Engineering grading of weathered granite: Engineering Geology, v. 12, p. 345-374.

Dunn, I. S., Anderson, L. R., and Kiefer, F. W., 1980, Fundamentals of geotechnical analysis: New York, John Wiley and Sons, Inc., 414 p.

Garwood, N. C., Janos, D. P., and Brokaw, Nicholas, 1979, Earthquake-caused landslides: a major disturbance to tropical forests: Science, v. 205, no. 4410, p. 997-999.

Gibbs, J. F., Fumal, T. E., Borchardt, R. D., and Roth, E. F., 1977, In-situ measurements of seismic velocities in the San Francisco Bay region: Part III: U.S. Geological Survey Open-File Report 77-850, 143 p.

Harp, E. L., Wilson, R. C., Wieczorek, G. F., and Keefer, D. K., 1978, Landslides from the February 4, 1976, Guatemala earthquake—Implications for seismic hazard reduction in the Guatemala City area: International Conference on Microzonation, 2d, San Francisco, Calif., 1978, Proceedings, v. 1, p. 351-366.

Harp, E. L., Wilson, R. C., and Wieczorek, G. F., 1981, Landslides from the February 4, 1976, Guatemala earthquake: U.S. Geological Survey Professional Paper 1204–A, p. A1–A35.

Herd, D. G., 1978, Neotectonic framework of central coastal California and its implications to microzonation of the San Francisco Bay region: International Conference on Microzonation, 2d, San Francisco, Calif., 1978, Proceedings, v. 1, p. 231-240.

Hoek, Evert, and Bray, John, 1977, Rock-slope engineering: London, The Institution of Mining and Metallurgy, 402 p.

Housner, G. W., and Trifunac, M. D., 1967, Analysis of accelerograms—Parkfield earthquake: Seismological Society of America Bulletin, v. 57, no. 6, p. 1193-1220.

Keefer, D. K., 1984, Landslides caused by earthquakes: Geological Society of America Bulletin, v. 95, p.406-421.

Keefer, D. K., Wieczorek, G. F., Harp, E. L., and Tuel, D. H., 1978, Preliminary assessment of seismically induced landslide susceptibility: International Conference of Microzonation, 2d, San Francisco, Calif., 1978, Proceedings, v. 1, P. 279-290.

Lambe, T. W., and Whitman, R. V., 1969, Soil mechanics: New York, John Wiley and Sons, Inc., 553 p.

Lajoie, K. R., Weber, G. E., Mathieson, Scott, and Wallace, James, 1979, Quaternary tectonics of coastal Santa Cruz and San Mateo Counties, California, as indicated by deformed marine terraces and alluvial deposits, *in* Weber, G. E., and others, Coastal tectonics and coastal geologic hazards in Santa Cruz and San Mateo Counties, California: Geological Society of America, Cordilleran Section, 75th Annual Meeting, San Jose, Calif., 1979, Field Trip Guide, p. 61-80.

Morton, D. M., 1975, Seismically triggered landslides in the area above the San Fernando Valley, *in* The San Fernando, California, earthquake of February 9, 1971: U.S. Geological Survey Professional Paper 733, p. 99-104.

Neumann, Frank, and Cloud, W. K., 1955, Strong-motion records of the Kern County earthquakes, *in* Oakeshott, G. B., editor, Earthquakes in Kern County during 1952: California Division of Mines Bulletin 171, p. 205-210.

Newmark, N. M., 1965, Effects of earthquakes on dams and embankments: Geotechnique, v. 15, no. 2, p. 139-160.

Sarma, S. K., 1975, Seismic stability of earth dams and embankments, Geotechnique, v. 25, no. 4, p. 743-761.

Seed, H. B., and Goodman, R. E., 1964, Earthquake stability of slopes of cohesionless soils: American Society of Civil Engineers, Soil Mechanics and Foundations Division Journal, v. 90, no. SM6, p. 43-73.

Sitar, Nicholas, and Clough, G. W., 1983, Seismic response of steep slopes in cemented soils: American Society of Civil Engineers, Geotechnical Engineering Division Journal, v. 109, no. GT2, p. 210-227.

Skempton, A. W., and Hutchinson, J. N., 1969, Stability of natural slopes and embankment foundations: International Conference on Soil Mechanics and Foundation Engineering, 7th Mexico City, 1969, State of the Art Volume, p. 291-340 .

Trifunac, M. D., and Hudson, D. E., 1971, Analysis of the Pacoima Dam accelerogram—San Fernando, California earthquake of 1971: Seismological Society of America Bulletin, v. 61, no